Gamma-ray Spectroscopy

Jordan Walsh - 120387836

Lab Report – PY3107

University College Cork

Department of Physics

March 2023

Gamma-ray Spectroscopy

1. Introduction

This document details the third practical attended on campus for PY3107. The experiment detailed throughout is ‘Gamma-ray Spectroscopy’.

1.1 Overview

Gamma ray spectroscopy is a powerful technique for analysing the energy spectra of gamma radiation emitted by radioactive isotopes. The analysis of gamma-ray spectra can provide important information about the structure and composition of materials, as well as their radiation properties. In this report, we use isotopes with known emission spectra to calibrate a Multi-Channel Analyser, use a scintillation detector and MCA to observe and record the emission spectra, and analyse the spectra of elements in detail.

1.2 Theory

Gamma rays are a type of electromagnetic radiation just like visible light, microwaves, x-rays, radio waves, etc. an electromagnetic wave (and thus a gamma-ray) can be described in terms of frequency, v, it’s energy, E, and wavelength, λ.

$$E = hv = h\frac{c}{\lambda}$$

Gamma rays are caused by the radioactive decay of atomic nuclei. certain atomic nuclei can exist in metastable ‘excited’ states which, when returning to their ground states, release a high-energy photon of definite energy in the form of a gamma ray. This process typically happens after a radioactive isotope has undergone beta decay to an excited isotope of a different element.

Just as elements exhibit characteristic electronic emission spectra which allows them to be identified and classified, (some) radioactive elements exhibit characteristic gamma ray emission spectra when undergoing radioactive decay, allowing them to be identified in a similar manner, aptly adopting the name ‘Gamma-ray Spectroscopy’.

2. Experimental Methods

Section 2, *Experimental Methods*, details procedure and experimental data produced from the experiment while providing brief discussion of reported data and fulfilling specified criteria of the lab brief.

2.1 Experimental Setup

Figure 2.1.1 shows a schematic representation of the apparatus used to detect gamma rays. The detector used in this experiment is a scintillation counter, which is capable of detecting gamma rays and distinguishing gamma-rays of various energies. It transforms the high energy photon absorbed into a fluorescence signal that is read by a photomultiplier connected to the base of the scintillator. The amplitude of the output pulses from such a detector is proportional to the energy of the detected gamma rays. A specialised computer program was used to read and record the detected gamma rays, which displayed the data as it was being collected in terms of impulses per channel (each channel representing a distinguishable energy as detected by the scintillation counter). This required calibration; a map from channel to energy in order to comprehend and analyse data in later parts of this report. The calibration is documented in section 2.2.

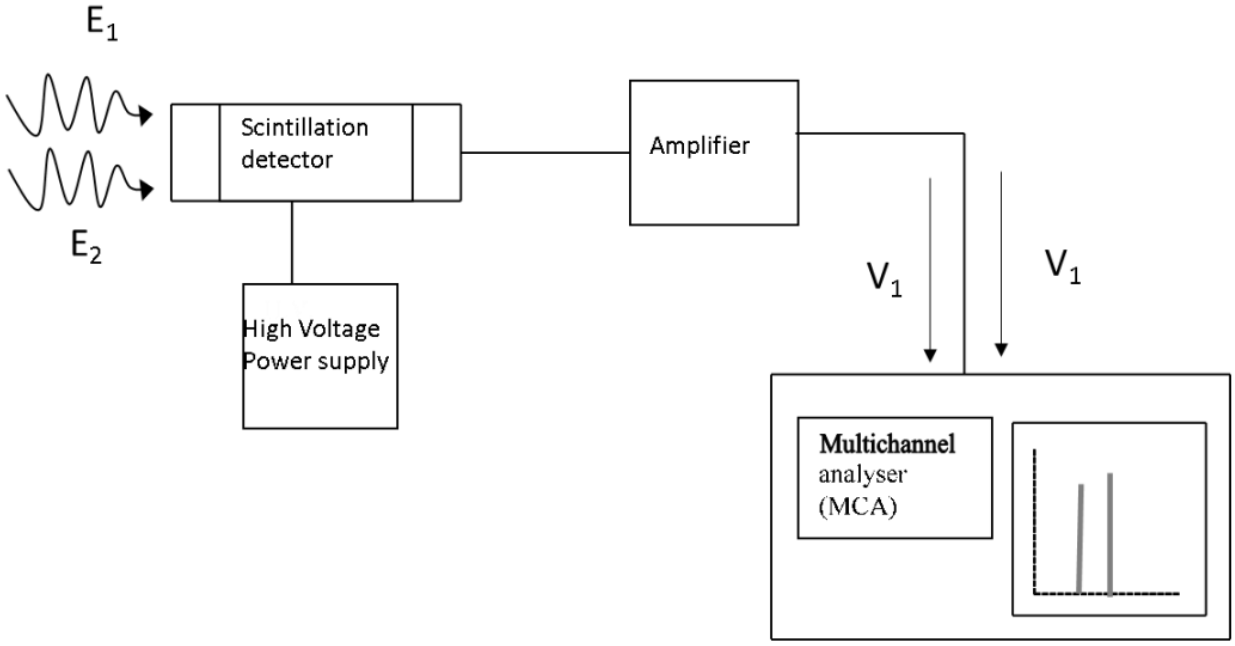

Fig 2.1.1 [1] – Apparatus used to detect gamma rays (schematic representation)

2.2 Calibration of the MCA

Three radiation sources, ^{60}Co, ^{137}Cs and ^{57}Co, which had a total of four known distinct energy peaks in their spectra, were used to calibrate the MCA channels to energy values in MeV. The elements were used in the order specified in the lab brief so that ^{60}Co, which had the highest energy peak at 1.33MeV, could have this peak calibrated with a high channel number on the MCA.

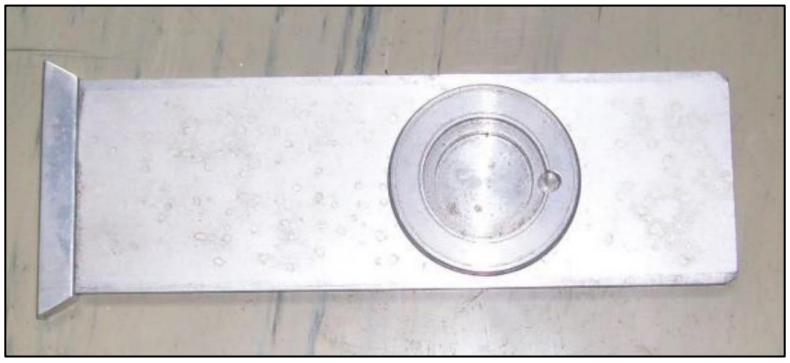

Fig 2.2.1 – scintillation detector holder (Radioactive isotopes placed in circular dish)

The ^{60}Co sample was first placed in its holder and inserted into the scintillation detector. The system and software were left to run for 2 minutes to allow sufficient data to be collected. The ^{60}Co sample required the most repeat attempts as when the energy spectrum was observed initially it was clear that the initial bias voltage of 0.6kV was too low and thus resulted in a low channel number for the 1.33MeV peak. To account for this, the bias voltage was slowly increased (but not above 1.2kV) until the 1.33MeV peak corresponded to a high channel number (recommended between 3000 and 3500). The respective channel numbers of the 1.33MeV and 1.17MeV peaks were recorded and the process was repeated for ^{137}Cs and ^{57}Co sources without changing the bias voltage.

Using the 4 values/channel numbers determined according to the peaks visible in the data, a calibration curve can be determined to be used throughout the rest of the experiment.

As an additional step, and to further represent the true nature of the isotopes, a background spectrum was recorded with the intention of subtracting the corresponding spectrum from following readings. All spectrums were recorded over a period of 120 seconds using the 'timed run' feature of the MCA computer interface. Experimental Data is shown in section 2.2.1. *Note to marker: due to an unknown technical error, the peaks of 60Co could not be fit between the reccomended channel numbers (3000-3500). This did not negatively effect results produced.*

2.2.1 Experimental Data

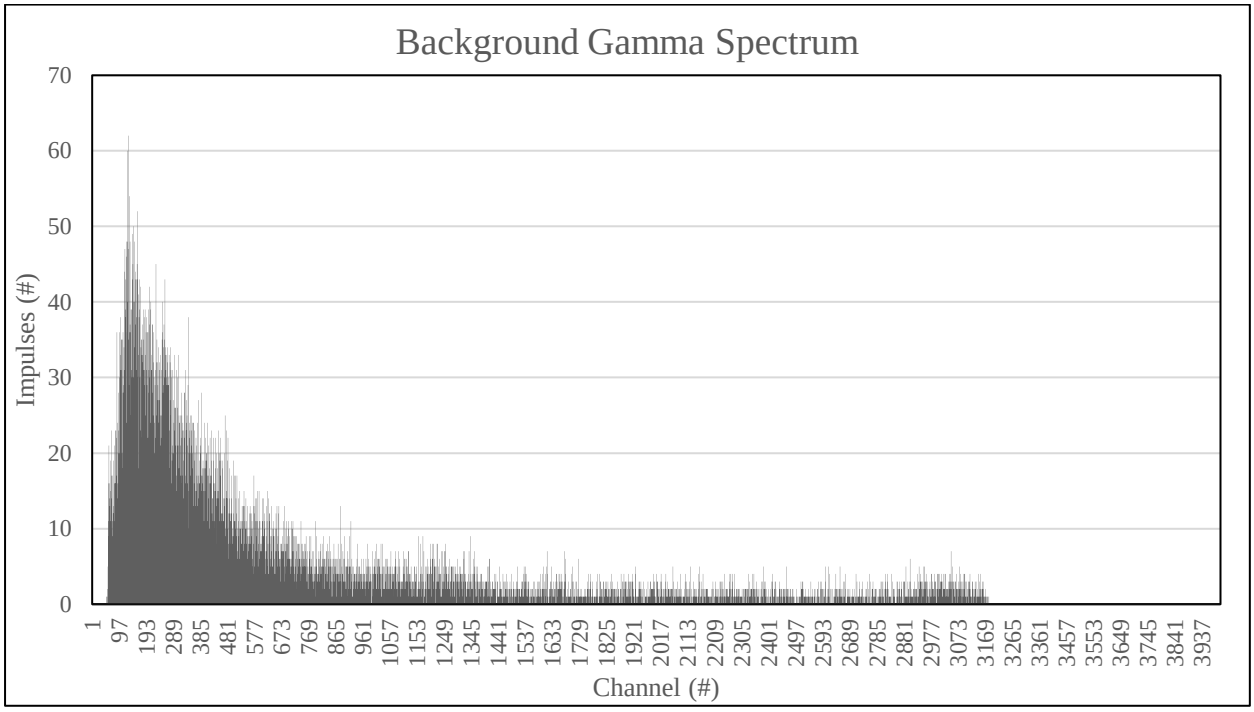

Fig 2.2.1 | Background spectrum | Raw Data | Impulses vs. Channel # | 120s

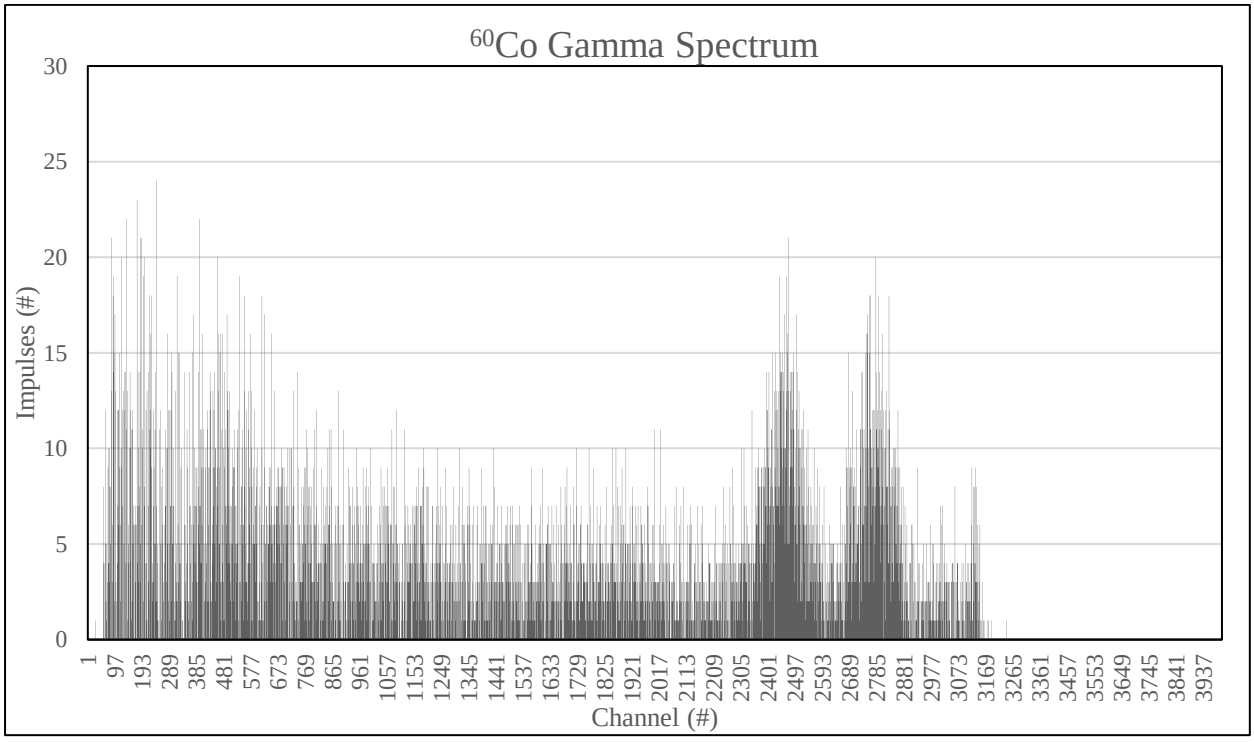

Fig 2.2.2 | ^{60}Co Spectrum | Background Radiation Subtracted | Impulses vs. Channel # | 120s

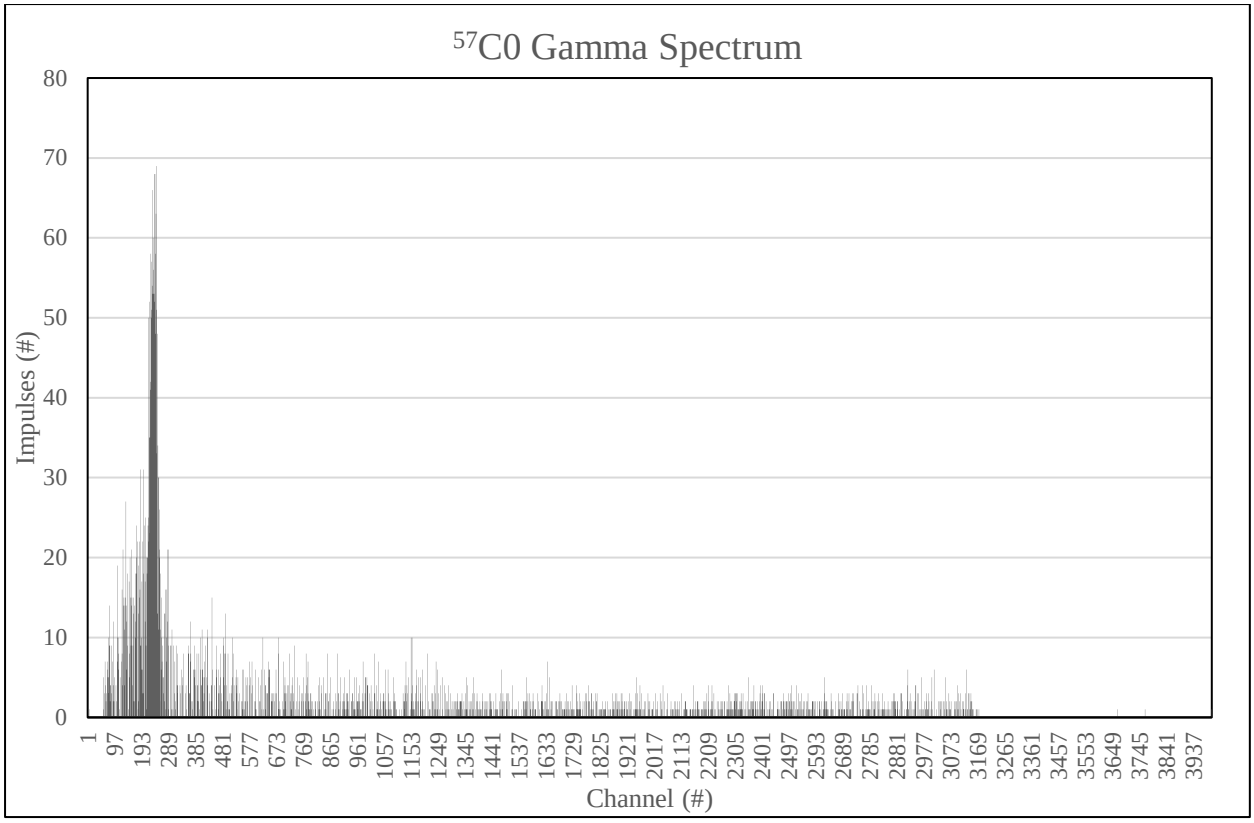

Fig 2.2.3 | ^{57}Co Spectrum | Background Radiation Subtracted | Impulses vs. Channel # | 120s

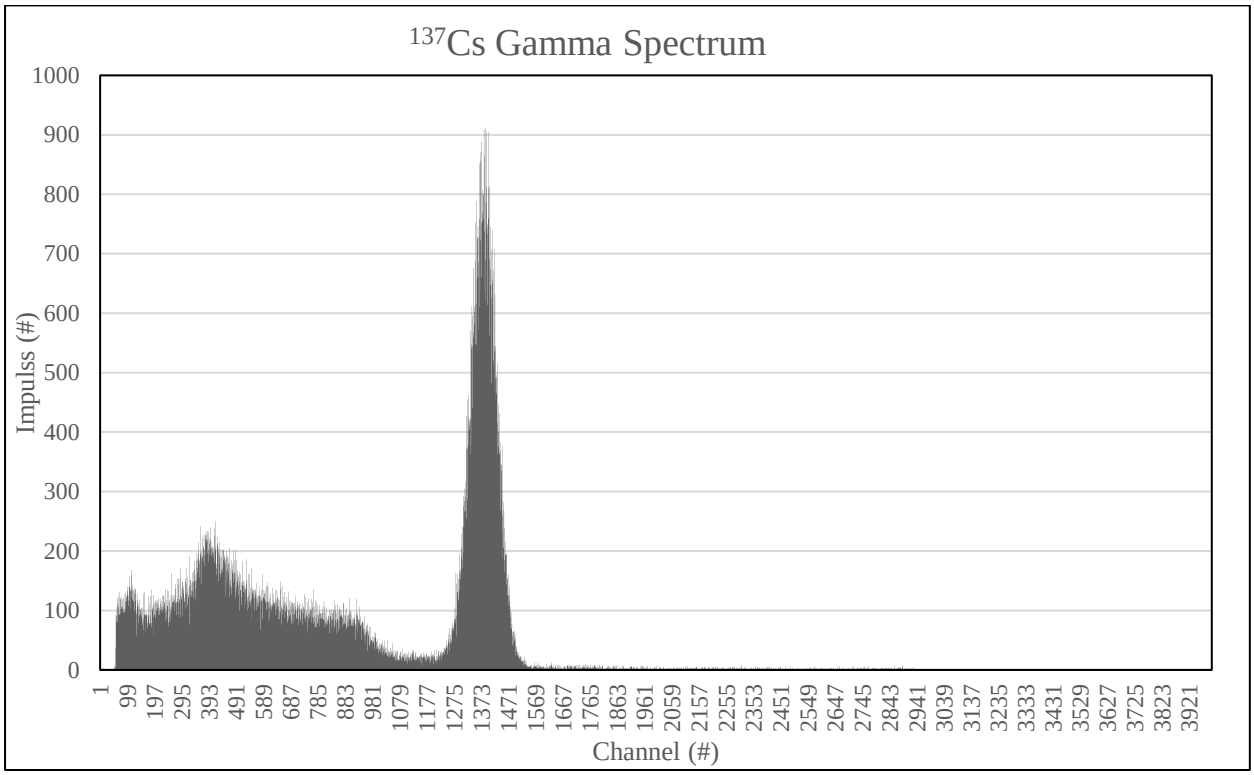

Fig 2.2.3 | ^{137}Cs Spectrum | Background Radiation Subtracted | Impulses vs. Channel # | 120s

2.2.2 Calculations / Error Analysis

Isotope	Channel #	FWHM #	E_{peak} MeV	E_{peak} eV
60Co	2788	172	1.33	1330000
	2463	248	1.17	1170000
137Cs	1398	102	0.662	662000
57Co	235	37	0.122	122000

Tab 2.2.1 | compilation of data from section 2.2.1

By taking the FWHM of the peaks (determined in Tab 2.2.1 by quantitative analysis of Figures 2.2.2 – 2.2.4) within the spectrums and assuming an approximate gaussian distribution of points, we can find an appropriate error in the channel number of the peaks using the fact that the FWHM of a gaussian is *approximately* equal to 2.4 standard deviations;

$$FWHM = 2\sqrt{2ln2}\,\sigma$$

$$\therefore \Delta Channel \equiv \sigma \approx \frac{FWHM}{2\sqrt{2ln2}}$$

As such we can modify our Table and determine approximate error bars for the calibration curve, as shown below in Figure 2.2.5 and Tab 2.2.2

Isotope	Channel #	FWHM #	E_{peak} MeV	E_{peak} eV	ΔChannel #
60Co	2788	172	1.33	1330000	73.19148936
	2463	248	1.17	1170000	105.5319149
137Cs	1398	102	0.662	662000	43.40425532
57Co	235	37	0.122	122000	15.74468085

Tab 2.2.2 | compilation of data from section 2.2.1 + Error bar approximations

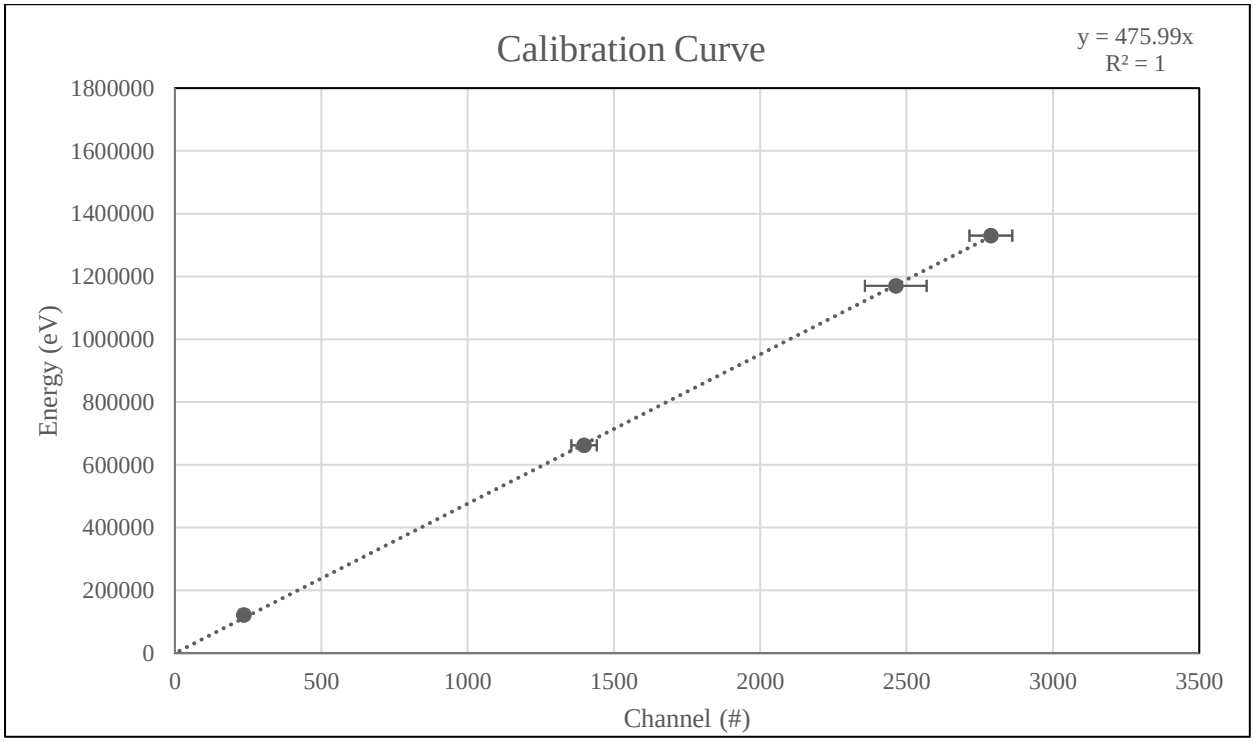

Fig 2.2.5 | Calibration Curve (complete with error bars) | s = 476

A brief numerical analysis and by fitting a curve between the error bars by eye, the maximum slope under the constraints posed by the determined errors are

$$\textit{Slope maximum} \approx 487 \rightarrow \Delta s = 11$$

$$\textit{Slope minimum} \approx 468 \rightarrow \Delta s = 8$$

producing a range of 19 in which the slope can var. The determined variation by excel interpolation, however, is $\Delta s = 1.64$. As shown in Figure 2.2.5, the correlation is effectively 100% when assuming a trend line through the origin and disregarding error bars. Given this, I would find it reasonable to assume that an appropriate (well, arguably generous) error in the slope can be determined from the mean of the two experimentally determined values above, i.e.

$$\Delta s = \frac{11 + 8}{2} = 6.88$$

$$\therefore s = 476 \pm 7$$

Therefore we can conclude a calibration constant, *k*, with an appropriate error of

$$k = (476 \pm 7)\ eV\ (Channel)^{-1}$$

2.3 Investigation of Emission Spectra of ^{226}Ra and ^{232}Th

In this section, the scintillation detector is used to detect gamma rays emitted from ^{226}Ra and ^{232}Th sources separately. A 'count vs. channel' graph was obtained for each source, and the peaks of the graphs were carefully noted. Using the equation of the calibration curve determined earlier, the channel numbers were converted to corresponding energy values in eV. The obtained photopeak values are compared to literature values. Through this analysis, we aim to gain a better understanding of the accuracy and reliability of gamma ray spectroscopy as a tool for identifying and quantifying radioactive isotopes.

2.3.1 Experimental Data / Analysis

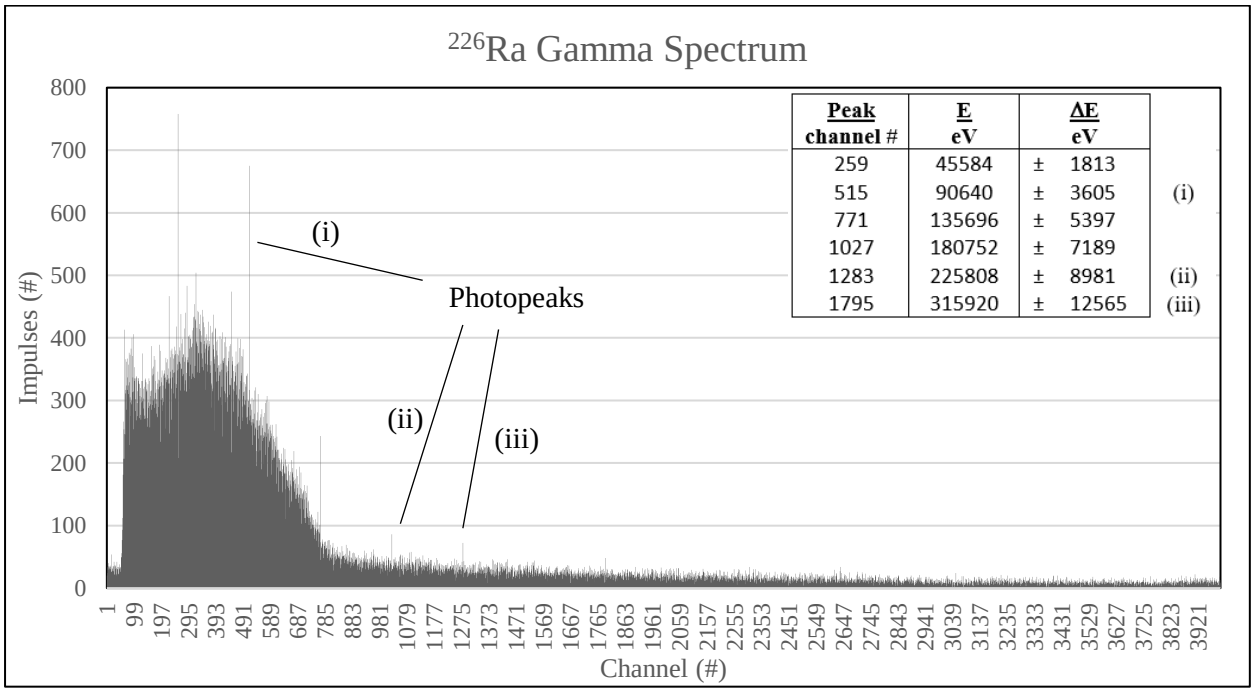

Fig 2.3.1 | ^{226}Ra Spectrum | Background Radiation Subtracted | Impulses vs. Channel # | 120s

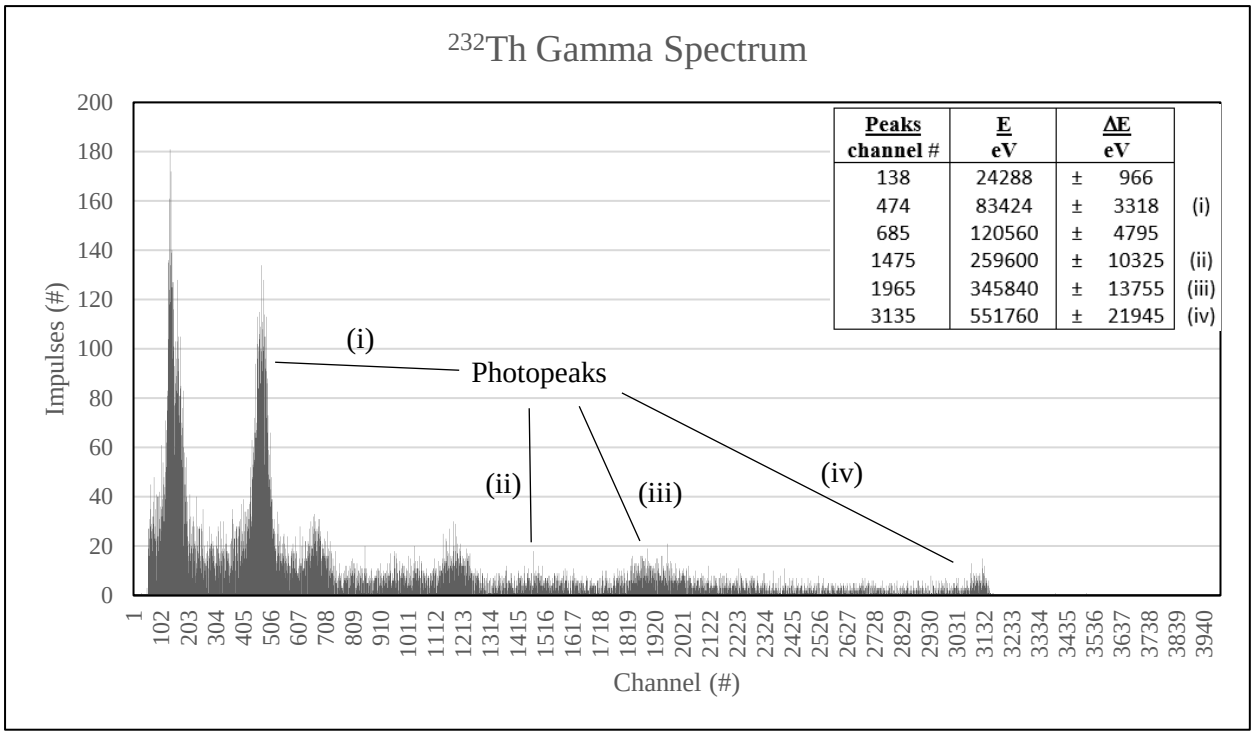

Fig 2.3.1 | ^{232}Th Spectrum | Background Radiation Subtracted | Impulses vs. Channel # | 120s

Peak channel #	E MeV	ΔE eV	
259	0.045584	± 1813	
515	0.090640	± 3605	(i)
771	0.135696	± 5397	
1027	0.180752	± 7189	
1283	0.225808	± 8981	(ii)
1795	0.315920	± 12565	(iii)

Tab 2.3.1 | 226Ra Photopeaks

Peaks channel #	E MeV	ΔE eV	
138	0.024288	± 966	
474	0.083424	± 3318	(i)
685	0.120560	± 4795	
1475	0.259600	± 10325	(ii)
1965	0.345840	± 13755	(iii)
3135	0.551760	± 21945	(iv)

Tab 2.3.2 | 232Th Photopeaks

There are a number of anomalies to be seen throughout both spectrums produced. In Tables 2.3.1 and 2.3.2 there are peaks labelled corresponding to those provided from literature as per the lab manual (exact sources not specified by lab manual). While they are not exactly at the expected energies, they are generally within or very close to the margin of error (which has been determined off the basis of the analysis in section 2.2.2).

As one can observe from the figures produced and the tables above, there are a number of peaks that are unaccounted for as listed in the manual. Particularly in the radium spectrum, whose form is barely comparable to literature (see section 3 for direct comparison). This may have been a systematic error with the equipment, the radium sample is directional, and did not comfortably insert into the scintillation counter setup, it would consistently get caught on the upper lip of the insertion point of the setup and tip to one side slightly – However, according to the manual, a puzzling spectrum was to be expected. The spectrum for Thorium-232, on the other hand, seems to be an excellent representation of what would be expected. See Discussion (Section 3) for more.

2.4 Detailed analysis of the spectra of ^{137}Cs and ^{60}Co

A detailed analysis of the Caesium and Cobalt-60 spectra obtained in section 2.3 is performed in this section. In addition to observing the energies of the photopeaks, we also examine the energies

of auxiliary peaks present in the data. These include the Compton edge and backscatter peak for each element. Furthermore, an analysis of the resolution of the spectrometer used in our measurements is performed.

Overall, this detailed analysis allowed us to explore the capabilities and limitations of gamma ray spectroscopy more fully as a tool for identifying and quantifying radioactive isotopes. By understanding the energy and resolution of various peaks in the spectra, we were able to improve the accuracy of our measurements and make more informed conclusions about the properties of the radioactive sources used in our experiment.

2.4.1 Analysis / Results

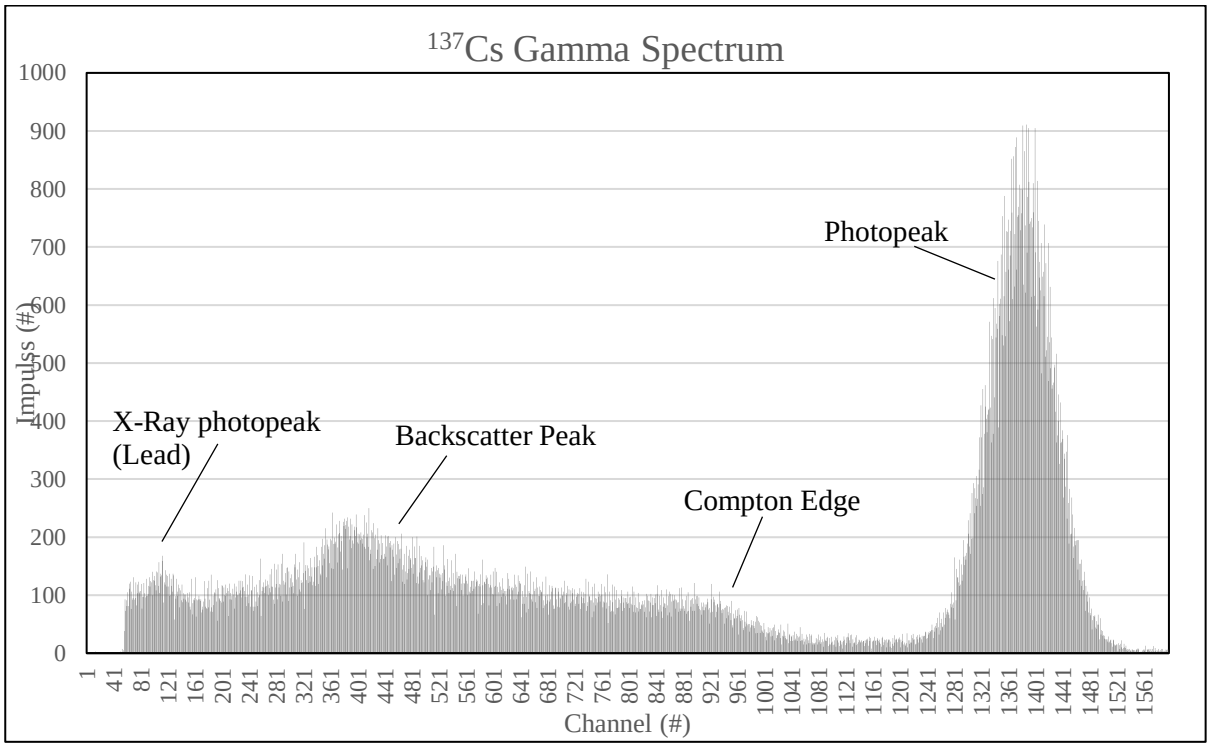

Fig 2.4.1 | ^{137}Cs Spectrum

Back Scatter Energy of ^{137}Cs (as provided by the lab manual):

$$E_{\gamma'} \cong \frac{E_\gamma}{1 + 2E_\gamma(1 - \cos\theta)}$$

Backscatter angle θ should correspond to $180° = \pi$, $E_\gamma(^{137}Cs) = 0.662\ MeV$

$$E_{\gamma'} \cong \frac{E_\gamma}{1 + 2E_\gamma\big(1 - (-1)\big)} = \frac{E_\gamma}{1 + 4E_\gamma}$$

$$\therefore E_{\gamma'} = \frac{0.662}{1 + 4(0.662)} = 0.181\ MeV$$

Compton Energy of ^{137}Cs:

Compton edge is the maximum energy imparted onto an electron from scattered gamma rays during Compton scattering. The energy of a recoil electron is given by the conservation of energy:

$$E_e = E_\gamma - E_{\gamma'}$$

$$\therefore E_e = 0.662\ MeV - 0.181\ MeV = 0.481\ MeV$$

The experimentally obtained values of these peaks (and a comparison to the theoretical) are shown below in Table 2.4.1.

Peak	E_{theory} MeV	Channel #	$E_{experimental}$ MeV	$\Delta E_{experimental}$ eV
Photopeak	0.662	1382	0.657832	± 9674
Backscatter	0.181	399	0.189924	± 2793
Compton Edge	0.481	902	0.429352	± 6314

Tab 2.4.1 | Comparison of theoretical energies and experimental (as determined from Fig 2.4.1)

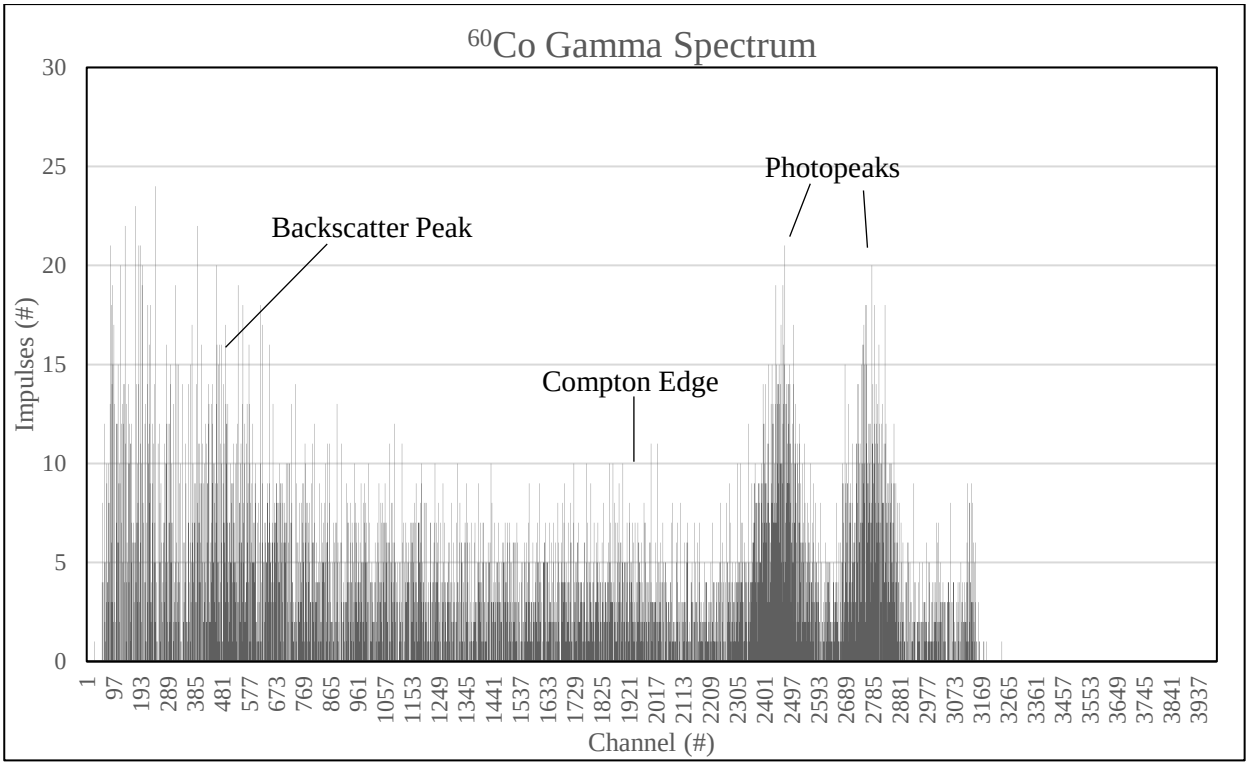

Fig 2.4.2 | ^{60}Co Spectrum

The method of analysis as determined for ^{137}Cs is identical for ^{60}Co. The results for ^{60}Co are as follows:

$$E_{\gamma'} = \frac{1.33}{1 + 4(1.33)} = 0.21\ MeV \quad \textbf{\textit{or}} \quad E_{\gamma'} = \frac{1.170}{1 + 4(1.170)} = 0.206\ MeV$$

$$E_e = 1.330 - 0.21 = 1.12\ MeV \quad \textbf{\textit{or}} \quad E_e = 1.17 - 0.206 = 0.964\ MeV$$

Peak	E_{theory} MeV	Channel #	$E_{experimental}$ MeV	$\Delta E_{experimental}$ eV
Photopeak	1.17	2463	1.172388	± 17241
	1.33	2788	1.327088	± 19516
Backscatter	0.21, 0.296	459	0.218484	± 3213
Compton Edge	1.12, 0.964	1899	0.903924	± 13293

Tab 2.4.2 | Comparison of theoretical energies and experimental (as determined from Fig 2.4.1)

Spectrometer Resolution:

In section 2.2.2 the FWHM was determined for the photopeaks of ^{137}Cs and ^{60}Co. Reusing the data obtained in section 2.2.2 here, we can determine an approximate spectrometer resolution.

$$R = \frac{\delta E}{E_{peak}} \equiv \frac{FWHM}{E_{peak}} = \frac{(\#\ Channels)k}{E_{peak}}$$

where k is the calibration constant determined in section 2.2.2.

Isotope	**Channel** #	**FWHM** #	**E_{peak}** **MeV**	**E_{peak}** **eV**
^{60}Co	2788	172	1.33	1330000
	2463	248	1.17	1170000
^{137}Cs	1398	102	0.662	662000
^{57}Co	235	37	0.122	122000

Tab 2.2.1 | compilation of data from section 2.2.1

As such, a brief analysis yields:

$$R(^{60}Co) = \frac{FWHM}{E_{peak}} = \frac{(172)(176\ eV)}{1.33\ MeV} = 0.023 \quad \textbf{\textit{and}} \quad \frac{(248)(176\ eV)}{1.17\ MeV} = 0.022$$

$$R(^{137}Co) = \frac{(102)(176\ eV)}{0.662\ MeV} = 0.027$$

$$R(^{57}Co) = \frac{(37)(176\ eV)}{0.112\ MeV} = 0.058$$

$$\rightarrow \bar{R} = \frac{0.058 + 0.027 + 0.022 + 0.023}{4} = 0.0325$$

$$\therefore R \approx 3.3\%$$

3. Discussion

Overall, this lab report serves as a comprehensive and detailed analysis of the use of gamma ray spectroscopy and attempts to provide valuable insights into the analysis of radioactive isotopes.

At a glance the experimentally determined results throughout are in line with expected values from theory. Particularly, the correlation between theory and measurements seen in section 2.2 (Detailed analysis of ^{137}Cs and ^{60}Co) is excellent. The values are qualitatively – and on this scale – effectively identical, even though some lie just outside the determined margin of error.

A part of this report that was not successful was the determined spectrum of ^{226}Ra. The spectrum shown in Figure 2.2.6 is barely comparable to that of other sources. There are distinct peaks that have been identified, however they are towered by peaks that serve as anomalies to the expected spectrum (as shown in Fig 3.1). As mentioned previously, this could have been due to a systematic error with the equipment (the radium pellet would get caught on insertion into the scintillon counter – see Figure 3.2 for context), however given that anomalies are mentioned to be expected in the lab brief, this may not be the case given the observed accuracy and determined spectra of all other measurements throughout this report. To add to this, the determined resolution of the system and results was 3.3%, which is surprisingly accurate given how qualitatively wide the

FWHM of the peaks seem at a glance. The nature of the anomalies are therefore difficult to accurately conclude, their existence however is undeniable.

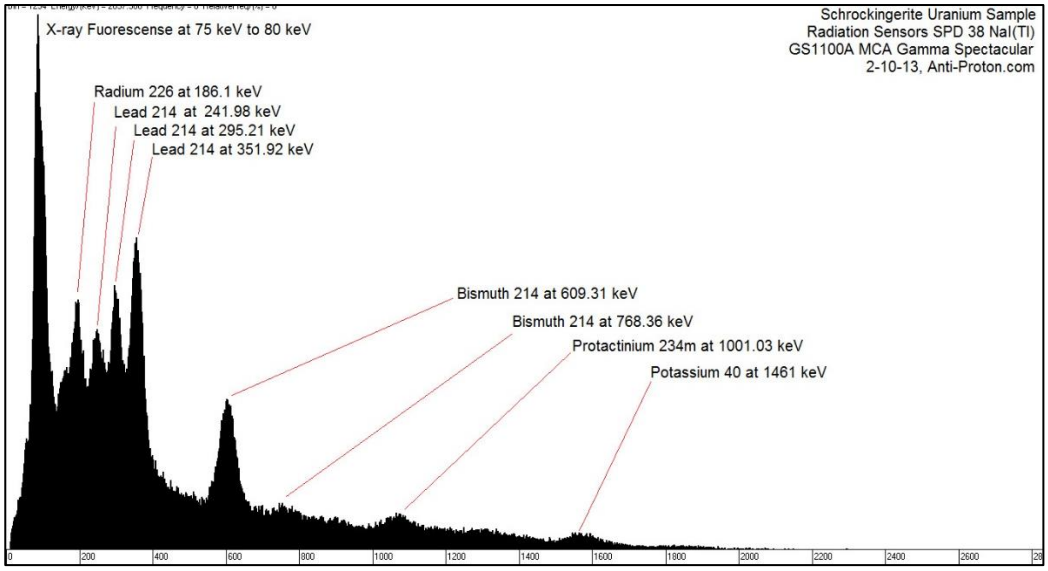

Fig 3.1 [2] | 226Ra Spectrum as determined by Cristoph Denk | See Reference for Source.

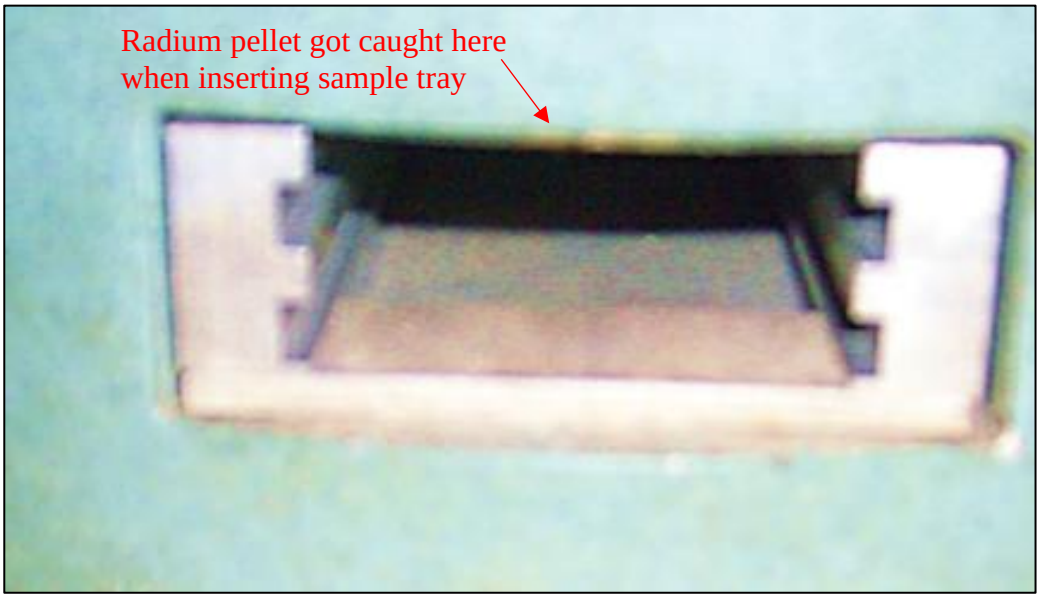

Fig 3.2 [1] | Radium pellet was larger than the allotted space for insertion – Sample would get caught on lip as indicated

On the flip side, within the same section we determined a ^{262}Th gamma spectrum which is undeniably the most reflective of theory and other experimental results. In Figure 3.3, a spectrum of ^{262}Th determined by an outside source is shown. This spectrum is effectively identical to that of which was determined here – the only difference being its wider range of detected energies and sharper, more exaggerated peaks. See Figure 3.3.

Although there was a subtraction of a background radiation spectrum (all spectrums were recorded over a 120 second period for consistency) – one of the main sources of error that affected results negatively throughout the report is noise entering the MCA from outside of the system. This is evident in all spectrums and made peaks in certain cases harder to detect within the data, particularly for the radium sample.

The spread of data near some peaks also made it difficult to accurately determine channel numbers, this mainly affected the ^{60}Co analysis – where the photopeaks are wide and the Compton edge and backscatter peaks are barely decipherable. However, the results deduced did, in conclusion, match that of theory appropriately.

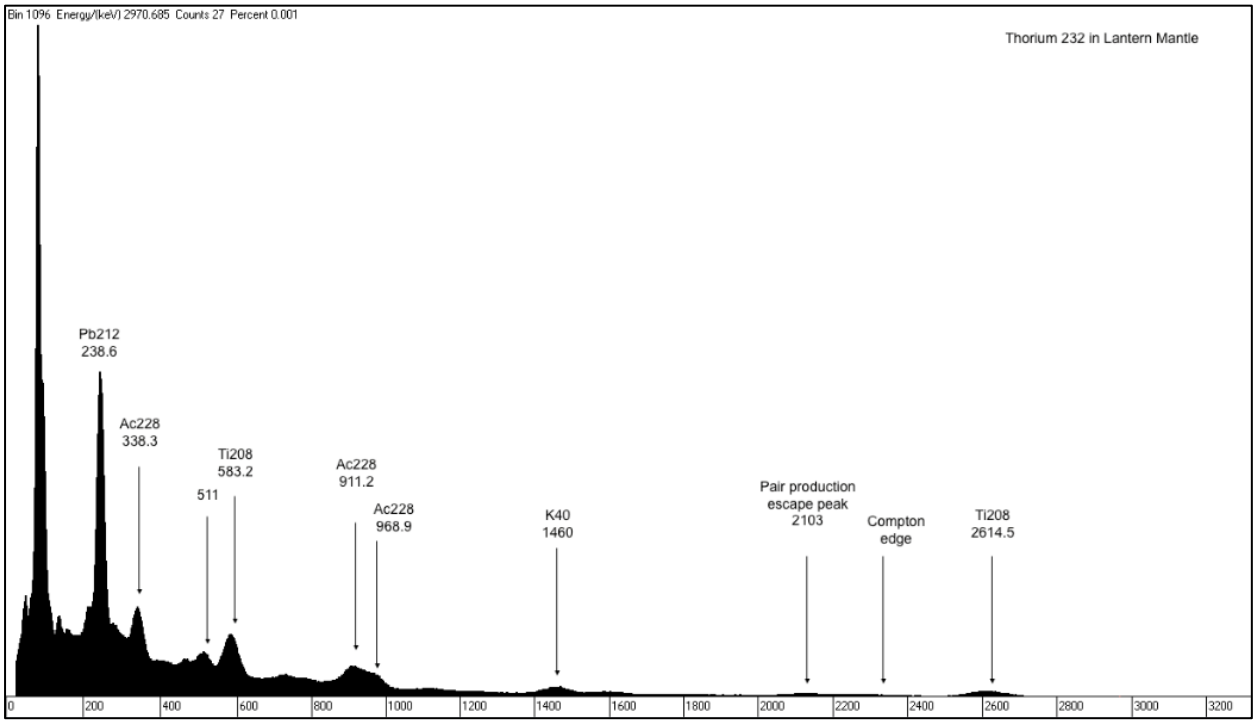

Fig 3.3 [3] | 226Ra Spectrum as determined by a third party| See Reference for Source.

References

[1] : Figure from UCC Department of Physics PY3107 Laboratory Manual

[2] : Cristoph Denk, Figure Source: https://www.gammaspectacular.com/blue/ra226-spectrum

[3] : Gamma Spectacular, Source: https://www.gammaspectacular.com/blue/th232-spectrum

Appendix 1 | Raw Data (no subtraction of background spectrum)

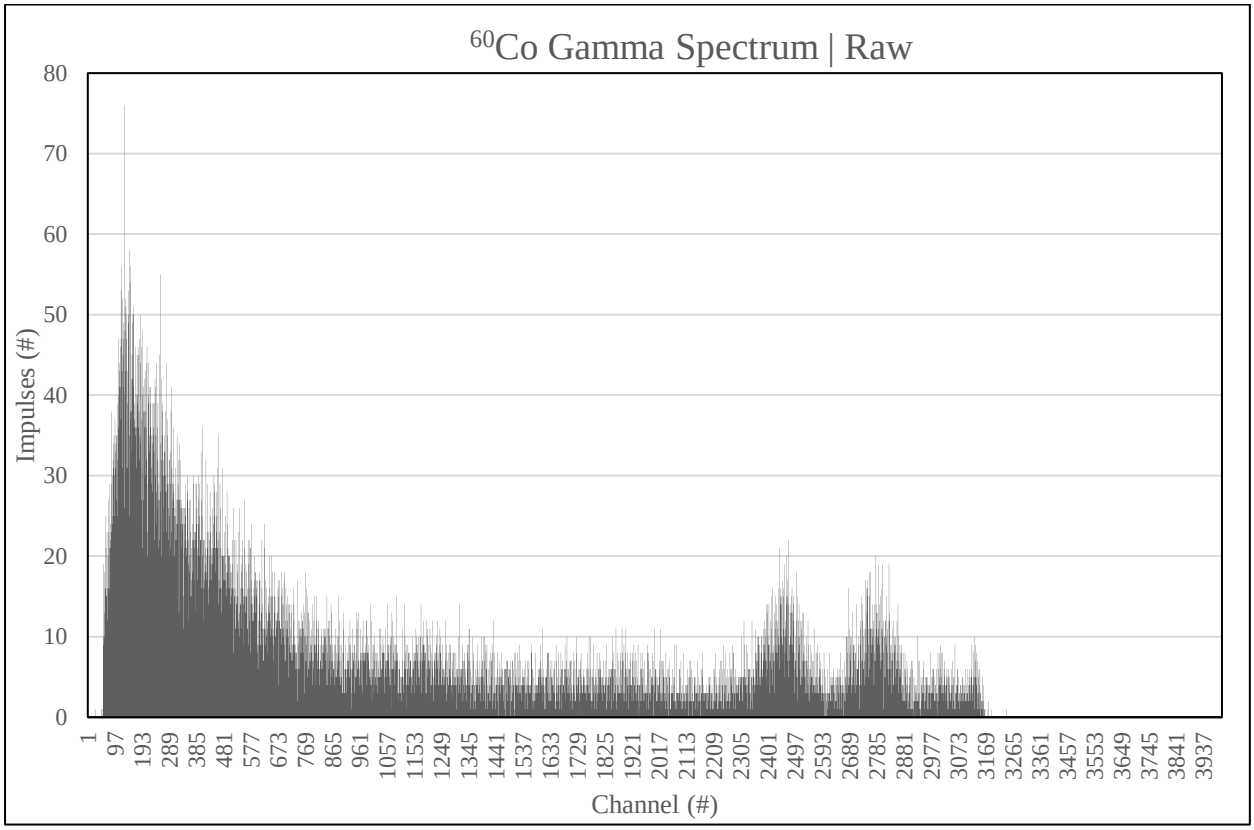

Fig A.1.1 | ^{60}Co Spectrum | Raw Data | Impulses vs. Channel # | 120s

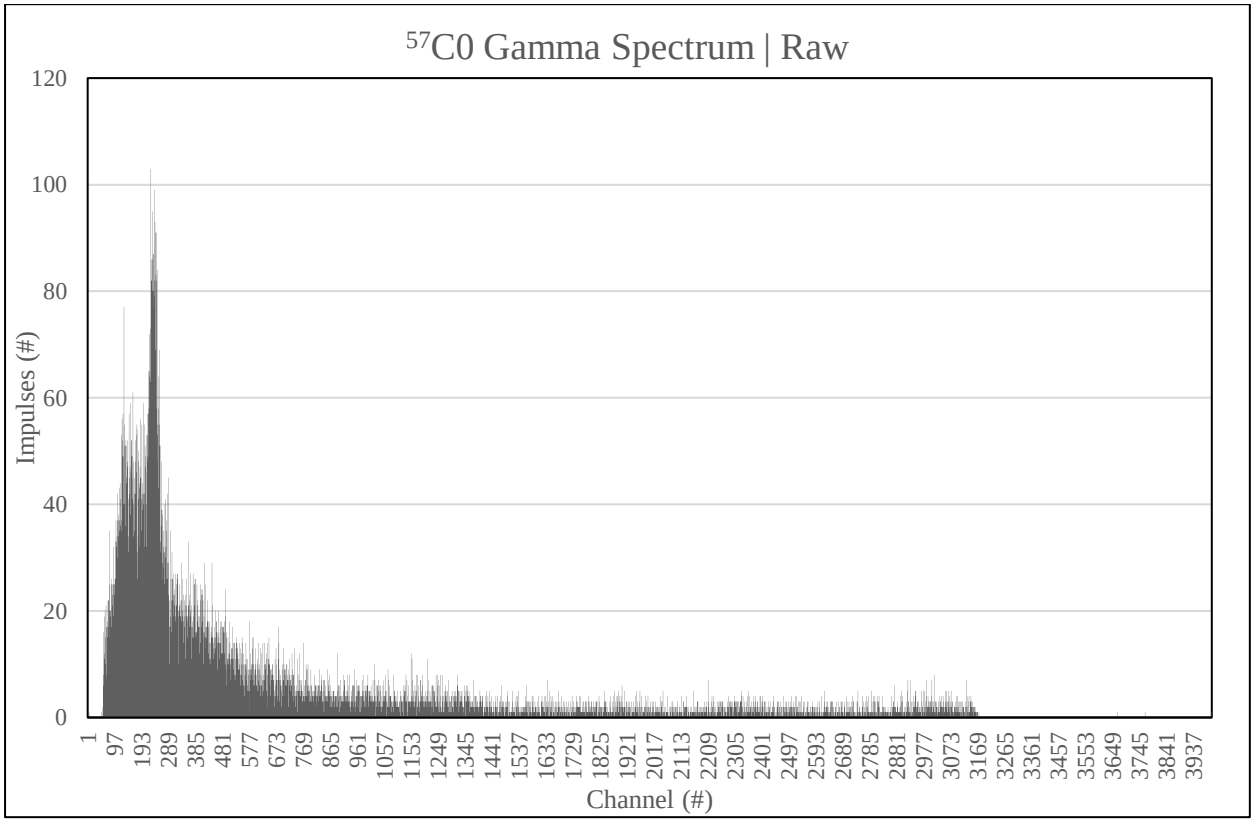

Fig A.1.2 | ^{57}Co Spectrum | Raw Data | Impulses vs. Channel # | 120s

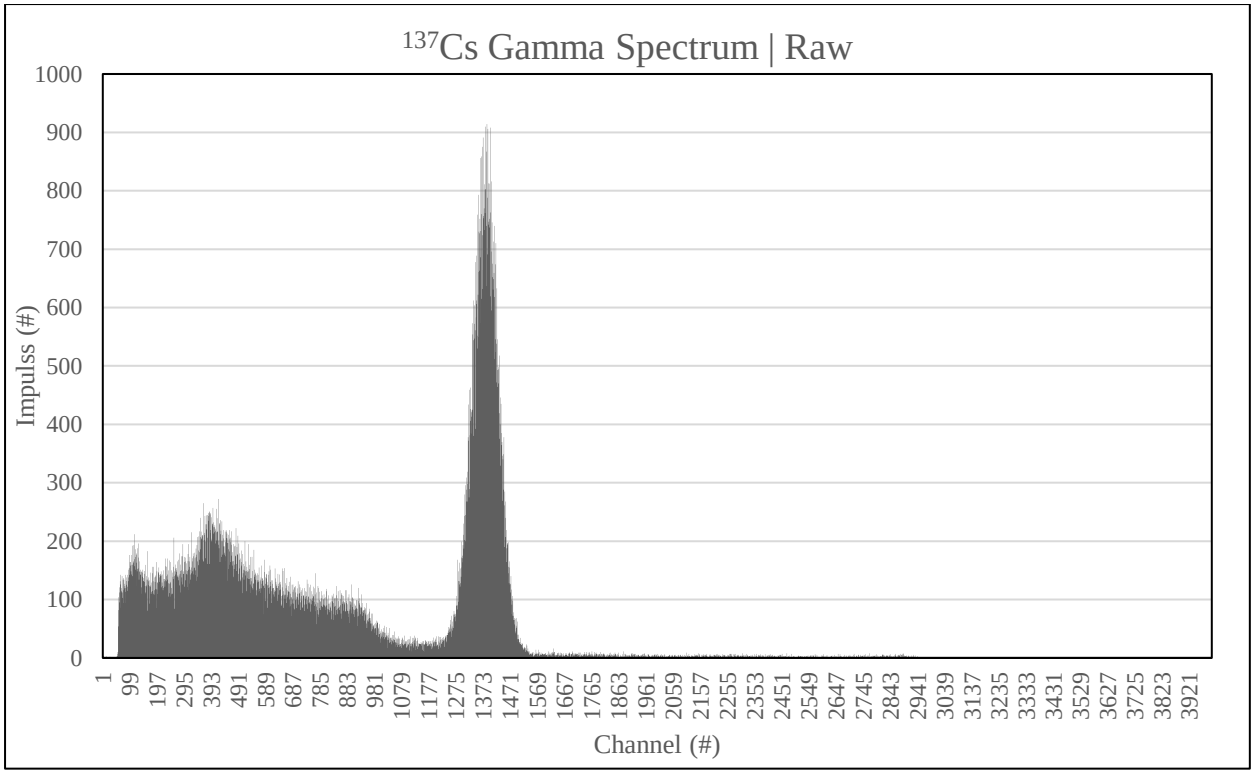

Fig A.1.3 | ^{137}Co Spectrum | Raw Data | Impulses vs. Channel # | 120s

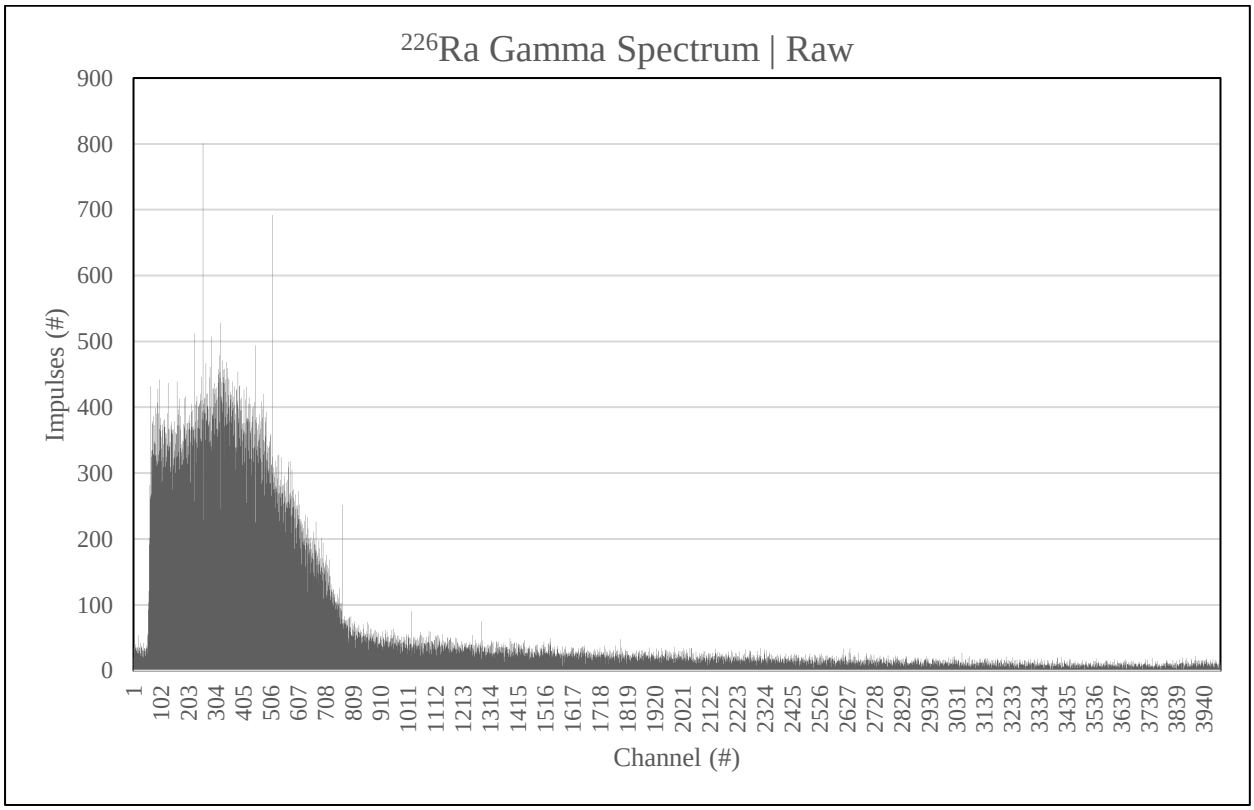

Fig A.1.4 | ^{226}Ra Spectrum | Raw Data | Impulses vs. Channel # | 120s